

Microstructure and mechanical properties of Mg-Gd-Y-Zr alloy cast by metal mould and lost foam casting

LI Ji-lin, CHEN Rong-shi, KE Wei

State Key Laboratory for Corrosion and Protection, Institute of Metal Research,
Chinese Academy of Sciences, Shenyang 110016, China

Received 25 September 2010; accepted 20 December 2010

Abstract: The microstructure and mechanical properties of Mg-10.1Gd-3.74Y-0.25Zr (mass fraction, %) alloy (GW104 alloy) cast by metal mould casting (MMC) and lost foam casting (LFC) were evaluated, respectively. It is revealed that different forming modes do not influence the phase composition of as-cast alloy. In the as-cast specimens, the microstructures are similar and composed of α -Mg solid solution, eutectic compound of α -Mg+Mg₂₄(Gd, Y)₅ and cuboid-shaped Mg₅(Gd, Y) phase; whereas the average grain size of the alloy produced by metal mould casting is smaller than that by lost foam casting. The eutectic compound of the alloy is completely dissolved after solution treatment at 525 °C for 6 h, while the Mg₅(Gd, Y) phase still exists after solution treatment. After peak-ageing, the lost foam cast alloy exhibits the maximum ultimate tensile strength of 285 MPa, and metal mould cast specimen 325 MPa at room temperature, while the tensile yield strengths of them are comparable. It can be concluded that GW104 alloy cast by lost foam casting possesses similar microstructure and evidently lower mechanical strength compared with metal mould cast alloy, due to slow solidification rate and proneness to form shrinkage porosities during lost foam casting process.

Key words: Mg-Gd-Y-Zr alloy; lost foam casting; metal mould casting; microstructure; mechanical property

1 Introduction

Magnesium alloys containing heavy rare earth elements, such as Gd and Y, are of high strength and low density, which make them be very attractive as structural materials in the aerospace and racing automotive industries where mass saving is of great value[1–2]. The equilibrium solid solubility of Gd in Mg is relatively high (4.53% in mole fraction, or 23.49% in mass fraction at 548 °C) and decreases exponentially with the decrease of temperature (0.61% in mole fraction or 3.82% in mass fraction at 200 °C). Thus, the Mg-Gd based alloys are prone to form supersaturated solid solution during the solidification, and the new strengthening precipitates would readily form by suitable aging treatment, which makes Mg-Gd alloys be ideal systems for precipitation hardening[3]. While Y and Zr added to Mg-Gd binary alloy will help to increase aging effect and to refine the grains[4]. Previously developed Mg-Gd-Y-Zr alloys exhibit higher specific strength at both room and elevated temperatures and better creep resistance than WE54 and QE22[5].

Currently, casting is still the main industrial forming method for magnesium alloys. Although magnesium alloys have been applied widely in aerospace, automobile and tele-communication industries, the lag of research and development on casting technology is still a bottleneck for their further application[6]. As is well known, lost foam casting (LFC) is a cost-effective, environment-friendly vital option to the conventional casting process for production of near-net shape castings with high quality. And the LFC process is widely employed by the automotive industry for making engine components[7]. Up to now, research of LFC has primarily concentrated on aluminum alloys, cast iron and steel[8–11], while little has been reported on magnesium alloys. It is anticipated that the combination of the lightest structural magnesium alloys with LFC process will bring a bright future for magnesium applications, especially in forming components with thin-wall, complex geometry, tight tolerance and smooth as-cast surface.

In the present work, a typical Mg-Gd-Y-Zr alloy (GW104) was cast by metal mould casting and lost foam casting, respectively. The as-cast microstructures, ageing

response and mechanical properties of the alloys at room temperature were studied comparatively in order to expose the differences between the two casting processes and discuss the reliability of lost foam casting process on Mg-Gd-Y-Zr alloy castings production.

2 Experimental

2.1 EPS pattern preparation

The foam material used in the lost-foam process is expanded polystyrene (EPS) with a density of 20 kg/m^3 . The foam was cut into different shapes by a foam cutting machine, and then assembled into a block shaped model, as shown in Fig.1. The model was then coated with a hydrated graphite blacking and the coating thickness was approximately 1 mm. Vacuum (30 kPa) assistance was employed during the casting procedure. Fig.1 illustrates the experimental set up for vacuum assisted mould filling.

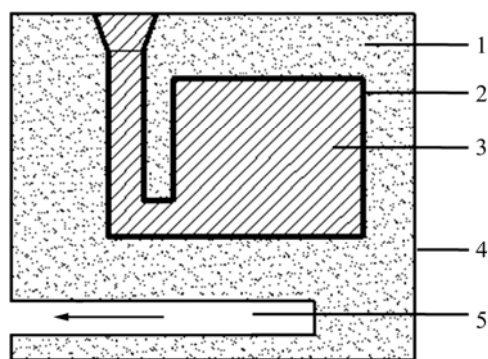


Fig.1 Experimental set up for vacuum assisted mould filling: 1—Quartz sand; 2—Permeable coating; 3—EPS pattern; 4—Sandbox; 5—Vacuum sucker

2.2 Alloy smelting, casting and heat treatment

The Mg-Gd-Y-Zr alloy was prepared by melting high pure Mg (>99.95%), Gd (>99%), Y (>99%) and Mg-30Zr (mass fraction, %) master alloy in an electric resistance furnace at $780\text{--}800 \text{ }^\circ\text{C}$ under protection of an RJ6 flux. The melt was poured firstly into a block shaped EPS pattern at about $780 \text{ }^\circ\text{C}$, and then poured into a mild steel mould preheated to $250 \text{ }^\circ\text{C}$. The chemical composition of the ingots was determined to be Mg-10.10Gd-3.74Y-0.25Zr (mass fraction, %) or Mg-1.61Gd-1.11Y-0.07Zr (mole fraction, %) by using inductively coupled plasma atomic emission spectroscopy (ICP-AES). Specimens cut from the cast ingots were solution treated at $525 \text{ }^\circ\text{C}$ for 6 h, quenched into water at about $25 \text{ }^\circ\text{C}$ and then subsequently aged at $225 \text{ }^\circ\text{C}$ for various periods of time.

2.3 Microstructure and mechanical property

The constituent phases of the alloy under different

conditions were identified by X-ray diffractometry (XRD) (Rigaku D/max 2400 X-ray diffractometer) with $\text{Cu K}\alpha$ radiation. Microstructures were observed by optical microscope (OM) and scanning electron microscope (SEM, Philips XL30 ESEM-FEG/EDAX). Samples for optical microscopy were etched in a solution of 5% (volume fraction) HNO_3 in ethanol after mechanical polishing to reveal grain boundaries. The mean grain size, d , was measured by the linear intercept method using the equation, $d = 1.74 L$, where L is the linear intercept of grain size determined by optical microscopy. No chemical etching was applied to specimens for SEM investigations. Compositions of phases were analyzed by energy dispersive X-ray spectrometry (EDS).

Vickers hardness testing was performed using 4.9 N load with a holding time of 15 s. The samples for tensile tests with a gauge length of 10 mm, width of 3.5 mm and thickness of 2 mm were cut by an electric-sparking wire-cutting machine from cast ingots. Tensile tests were conducted at room temperature with an initial strain rate of 10^{-3} s^{-1} on a universal testing machine. Four specimens were used for each test condition to ensure the reliability of data.

3 Results and discussion

3.1 Microstructures of Mg-Gd-Y-Zr alloy

The microstructures of the as-cast and solution-treated alloys are shown in Fig.2. It can be seen clearly that as-cast microstructures of Mg-Gd-Y-Zr alloys prepared by metal mould casting and lost foam casting are similar, with a network of eutectic compound distributing along the grain boundaries. Whereas the average grain sizes of the alloys cast by metal mould casting and lost foam casting are $108 \mu\text{m}$ and $216 \mu\text{m}$, respectively. The grain coarsening of the lost foam cast alloy is supposed to be caused by the slow solidification rate during casting process. And the microstructures of both the alloys are mainly composed of $\alpha\text{-Mg}$ solid solution, eutectic compound of $\alpha\text{-Mg}+\text{Mg}_{24}(\text{Gd}, \text{Y})_5$ and cuboid-shaped $\text{Mg}_5(\text{Gd}, \text{Y})$ phase, as can be seen in Fig.3(a), which is similar with previous study by HE et al[5]. After solution treated at $525 \text{ }^\circ\text{C}$ for 6 h the eutectic compound of the alloy was completely dissolved, while the $\text{Mg}_5(\text{Gd}, \text{Y})$ phase still exists after solution treatment, as shown in Fig.3(b).

The XRD patterns of as-cast alloys are shown in Fig.4(a). It can be confirmed that the phase constituents of LFC and MMC GW104 alloys are basically the same. The $\alpha\text{-Mg}$ peaks and some $\text{Mg}_{24}(\text{Gd}, \text{Y})_5$ peaks are observed in the alloys, which is consistent with the above microstructure observation. However, the $\text{Mg}_5(\text{Gd}, \text{Y})$ phase formed during the casting process is hardly detected because of the small volume fraction and the

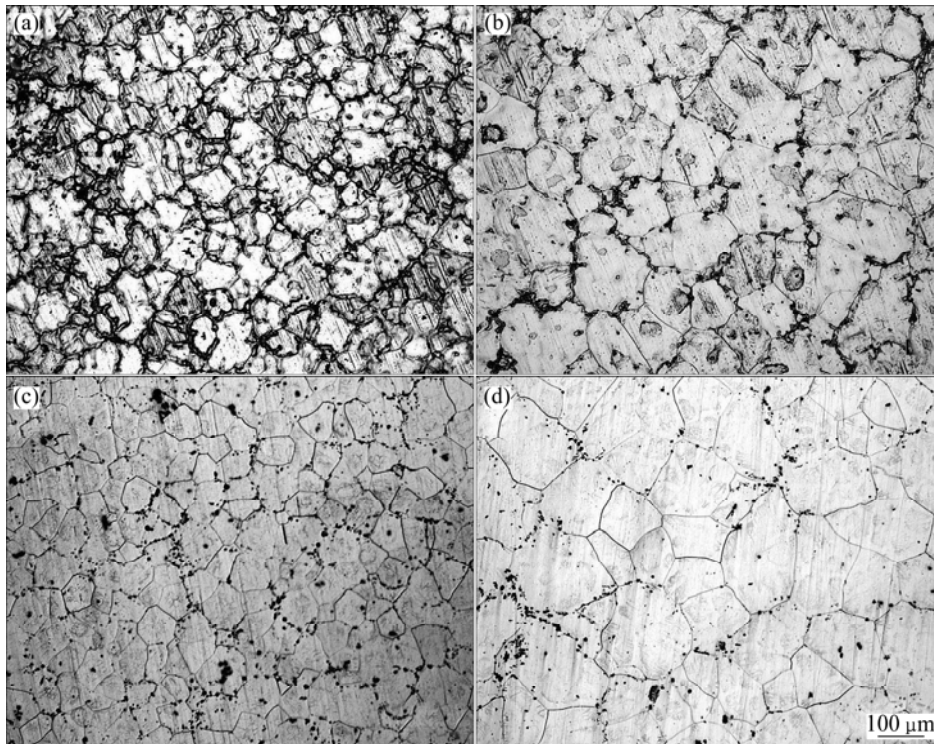


Fig.2 Microstructures of Mg-Gd-Y-Zr alloy: (a) As-cast MMC alloy; (b) As-cast LFC alloy; (c) Solution-treated MMC alloy; (d) Solution treated LFC alloy

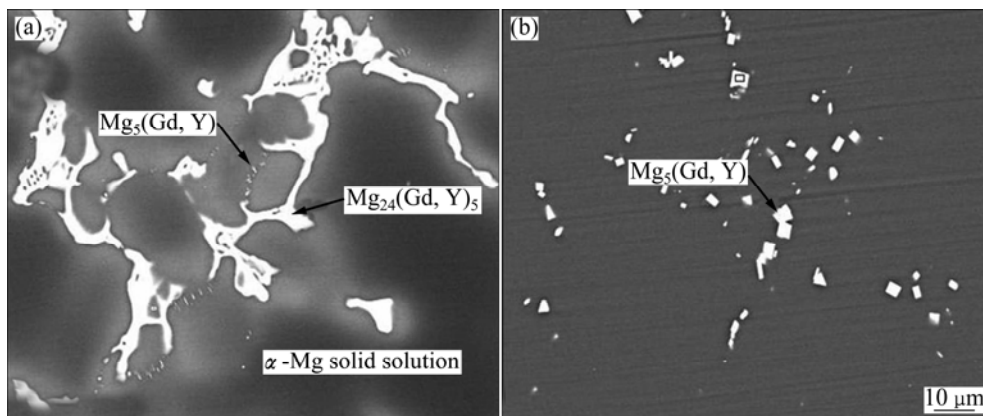


Fig.3 SEM images of LFC Mg-Gd-Y-Zr alloy: (a) As-cast sample; (b) Solution treated sample

limited particle size. After solution treatment, the $Mg_{24}(Gd, Y)_5$ peaks disappear, as shown in Fig.4(b), which is in agreement with the microstructure shown in Fig.3(b).

3.2 Age hardening response

Figure 5 shows the hardness curves of the Mg-Gd-Y-Zr alloys during aging treatment at 225 °C. As can be seen, the two alloys have similar age hardening response. Prior to aging, the initial hardness of the solution treated alloy is around HV72. During the aging treatment, the hardness starts to increase rapidly after an incubation period of about 1 h and then reaches the peak hardness of HV120 at about 24 h; while further aging

leads to a rapid decrease in hardness due to coarsening of the precipitates[12].

3.3 Mechanical properties

The typical tensile stress—strain curves of GW104 alloys under different conditions are shown in Fig.6. Compared with MMC specimens, the mechanical properties of LFC specimens are relatively low. The mechanical properties of GW104 alloys cast by metal mould casting and lost foam casting are listed in Table 1, in which we can see that the ultimate tensile strength (UTS) and fracture elongation (EL) of LFC specimens are remarkably lower than those of MMC specimens, while the tensile yield strengths (TYS) of the

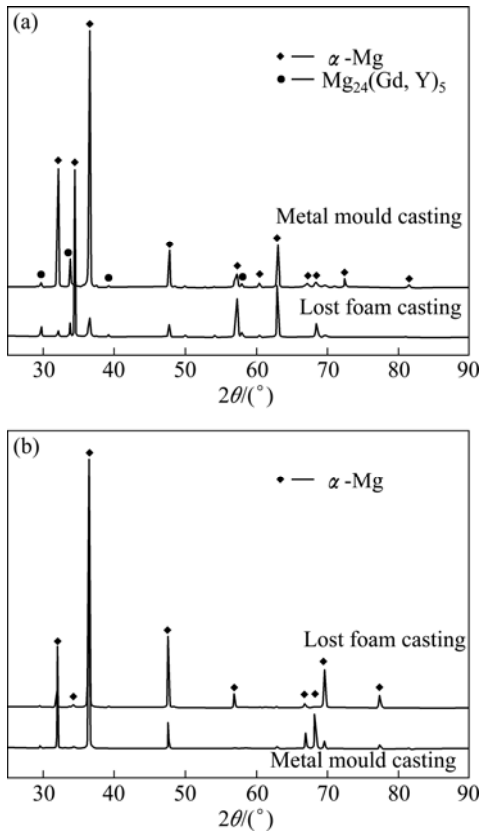


Fig.4 X-ray patterns of Mg-Gd-Y-Zr alloy in as-cast and solution treated conditions

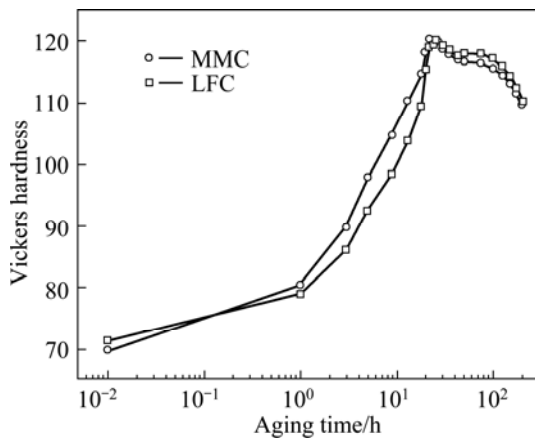


Fig.5 Aging hardening curves of Mg-Gd-Y-Zr alloy at 225 °C

specimens are comparable. This is in accordance with the previous research in aluminum castings[13].

According to the Hall-Petch relationship, the TYS of an alloy can be approximated as

$$\sigma_{ys} = \sigma_0 + kd^{-1/2} \quad (1)$$

where σ_{ys} is the tensile yield strength, k is the Petch parameter, and d is the mean grain size.

As for Mg-Gd-Y-Zr alloy, a k value of 188 MPa· $\mu\text{m}^{1/2}$ taken from a previous study[14] was used in this study. So the difference of TYS between LFC alloy

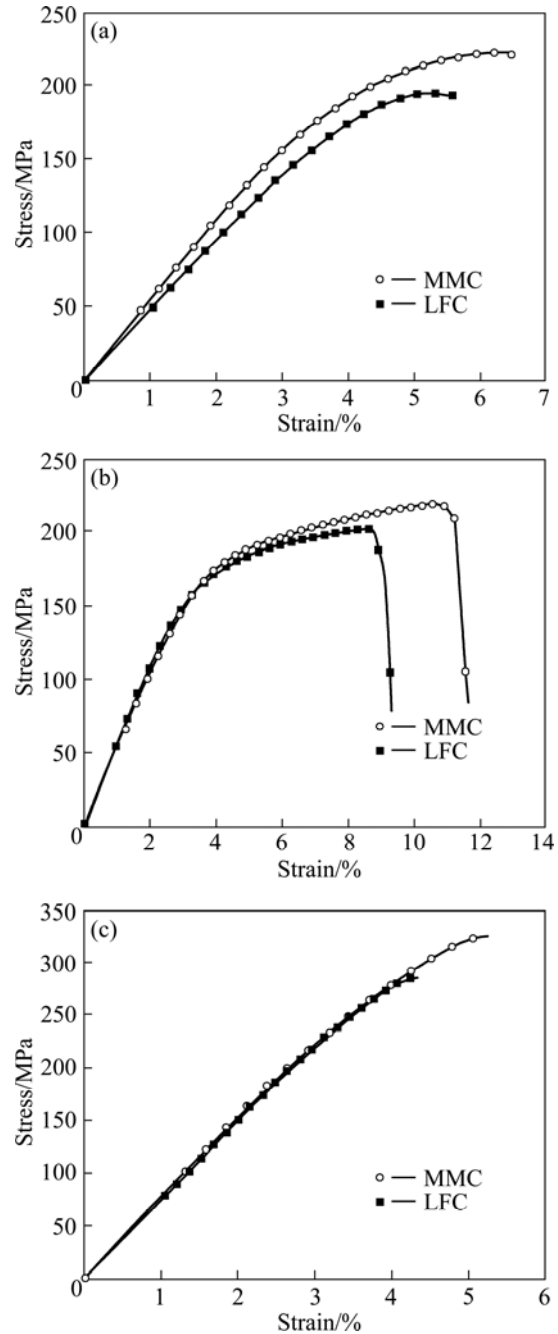


Fig.6 Typical nominal stress—strain curves of Mg-Gd-Y-Zr alloy under various conditions: (a) As-cast; (b) Solution treated; (c) Peak-aged

and MMC alloy can be calculated as

$$\Delta\sigma_{ys} = kd_1^{-1/2} - kd_2^{-1/2} = 188 \times (108^{-1/2} - 216^{-1/2}) = 5.3 \text{ MPa} \quad (2)$$

where d_1 and d_2 are the mean grain sizes of MMC and LFC specimens, respectively.

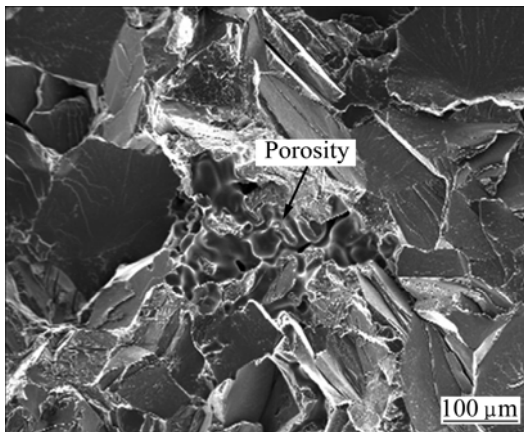
The results are in accordance with the experimental results, as listed in Table 1.

While the remarkable differences of the UTS and elongation between LFC and MMC specimens are most probably caused by the high porosity content in LFC specimens. Because the porosities in the alloy will

Table 1 Mechanical properties of Mg-Gd-Y-Zr alloy produced though different methods

Temper	MMC specimen			LFC specimen		
	UTS/ MPa	YS/ MPa	EL/ %	UTS/ MPa	YS/ MPa	EL/ %
As-cast	222	165	6.4	194	162	5.6
Solution-treated	219	144	11.6	202	136	9.3
Peak-aged	325	268	5.1	285	265	4.3

induce stress concentration, the stress concentration close to the porosities will initiate micro-cracks, while high density of micro-cracks will surely accelerate the fracture and reduce the ultimate tensile strength[15]. This may be approved by the fact that shrinkage porosities were detected on tensile-ruptured surfaces of EPC specimens shown in Fig.7, while no such defect was observed on tensile-ruptured surfaces of MMC specimens. So it is of great importance to reduce the content of porosities in lost foam coatings in order to improve their tensile strength.

**Fig.7** SEM image showing shrinkage porosity on tensile-ruptured surface of LFC Mg-Gd-Y-Zr alloy

4 Conclusions

1) The Mg-Gd-Y-Zr alloys (GW104 alloy) prepared by metal mould casting and lost foam casting have similar microstructures composed of α -Mg solid solution, eutectic compound of α -Mg+Mg₂₄(Gd, Y)₅ and cuboid-shaped Mg₅(Gd, Y) phase, but the grain size of MMC specimens is much smaller than that of LFC specimens.

2) The age hardening responses of the two alloys are basically the same. Both the LFC alloy and the MMC alloy reach their peak hardness after being aged at 225 °C for 24 h.

3) Due to the larger grain size, the tensile yield strength of peak-aged LFC Mg-Gd-Y-Zr alloy (265 MPa)

is slightly lower than that of MMC alloy (268 MPa). While the ultimate tensile strength of LFC Mg-Gd-Y-Zr alloy (285 MPa) is rather lower than that of MMC alloy (325 MPa), which may be caused by the high porosity content in LFC alloy.

References

- [1] ANYANWU I A, KAMADO S, KOJIMA Y. Aging characteristics and high temperature tensile properties of Mg-Gd-Y-Zr alloys[J]. *Materials Transactions*, 2001, 42(7): 1206–1211.
- [2] ANYANWU I A, KAMADO S, KOJIMA Y. Creep properties of Mg-Gd-Y-Zr alloys[J]. *Materials Transactions*, 2001, 42(7): 1212–1218.
- [3] NIE J F, GAO X, ZHU S M. Enhanced age hardening response and creep resistance of Mg-Gd alloys containing Zn[J]. *Scripta Materialia*, 2005, 53(9): 1049–1053.
- [4] WANG J, MENG J, ZHANG D P, TANG D X. Effect of Y for enhanced age hardening response and mechanical properties of Mg-Gd-Y-Zr alloys[J]. *Materials Science and Engineering A*, 2007, 456(1–2): 78–84.
- [5] HE S M, ZENG X Q, PENG L M, GAO X, NIE J F, DING W J. Microstructure and strengthening mechanism of high strength Mg-10Gd-2Y-0.5Zr alloy[J]. *Journal of Alloys and Compounds*, 2007, 427(1–2): 316–323.
- [6] LIU Z L, HU J Y, WANG Q D, DING W J, ZHU Y P, LU Y Z, CHEN W Z. Evaluation of the effect of vacuum on mold filling in the magnesium EPC process[J]. *Journal of Materials Processing Technology*, 2002, 120(1–3): 94–100.
- [7] KANNAN P, BIERNACKI J J, VISCO P D. A review of physical and kinetic models of thermal degradation of expanded polystyrene foam and their application to the lost foam casting process[J]. *Journal of Analytical and Applied Pyrolysis*, 2007, 78(1): 162–171.
- [8] GRIFFITHS W D, DAVIES J P. The permeability of lost foam pattern coatings for Al alloy castings[J]. *Journal of Materials Science*, 2008, 43(16): 5441–5447.
- [9] LI Z L, JIANG Y H, ZHOU R, LU D H, ZHOU R F. Dry three-body abrasive wear behavior of WC reinforced iron matrix surface composites produced by V-EPC infiltration casting process[J]. *Wear*, 2007, 262(5–6): 649–654.
- [10] SANTOS D D, VROOMEN U, BUHRIG-POLACZEK A. ADI lost-foam: Synergy of process and material[J]. *Advanced Engineering Materials*, 2007, 9(4): 259–264.
- [11] KUMAR S, KUMAR P, SHAN H S. Parametric optimization of surface roughness castings produced by evaporative pattern casting process[J]. *Materials Letters*, 2006, 60(25–26): 3048–3053.
- [12] WEI L Y, DUNLOP G L, WESTENGEN H. Age hardening and precipitation in a cast magnesium rare-earth alloy[J]. *Journal of Materials Science*, 1996, 31(2): 387–397.
- [13] EADY J A, SMITH D M. The effect of porosity on the tensile properties of aluminium castings[J]. *Materials Forum*, 1986, 9(4): 217–23.
- [14] GAO L, CHEN R S, HAN E H. Microstructure and strengthening mechanisms of a cast Mg-1.48Gd-1.13Y-0.16Zr (at.%) alloy[J]. *Journal of Alloys and Compounds*, 2009, 481(1–2): 379–384.
- [15] CACERES C H, SELLING B I. Casting defects and the tensile properties of an Al-Si-Mg alloy[J]. *Materials Science and Engineering A*, 1996, 220(1–2): 109–116.

金属型铸造和消失模铸造 Mg-Gd-Y-Zr 合金的组织结构和力学性能

李吉林, 陈荣石, 柯伟

中国科学院 金属研究所 金属腐蚀与防护国家重点实验室, 沈阳 110016

摘要: 研究金属型铸造和消失模铸造 Mg-10.1Gd-3.74Y-0.25Zr (质量分数, %)合金的组织结构和力学性能。结果表明: 采用两种铸造工艺得到的合金具有相似的铸态组织, 均由 α -Mg 固溶体相、 α -Mg+Mg₂₄(Gd,Y)₅ 共晶相和立方状 Mg₅(Gd, Y)相组成; 但金属型铸造合金的晶粒尺寸明显小于消失模铸造合金。经 525 °C, 6 h 固溶处理后, 合金中的共晶相完全溶入基体中, 而立方状 Mg₅(Gd, Y)相仍然存在。固溶处理后的合金在 225 °C 时效处理 24 h 后达到硬化峰值。经过时效处理后, 消失模铸造合金和金属型铸造合金的室温抗拉强度分别提高到 285 MPa 和 325 MPa, 但两者的屈服强度相差不大。与金属型铸造相比, 消失模铸造过程中合金的冷却速度相对较慢, 而且消失模铸造 Mg-Gd-Y-Zr 合金铸件更容易产生缩松等铸造缺陷, 这是造成两种合金强度差异的主要原因。

关键词: Mg-Gd-Y-Zr 合金; 消失模铸造; 金属型铸造; 组织结构; 力学性能

(Edited by LI Xiang-qun)